京都大学防災研究所年報 第 61 号 B 平成 30 年
DPRI Annuals, No. 61 B, 2018

Investigation of Relationship between RDCA Index Using Himawari-8 Data and Radar Estimated Hydrometeor Type aloft Considering the Stage of Cumulus Cloud

Wendi HARJUPA[(1)], Eiichi NAKAKITA , Yasuhiko SUMIDA[(2)]
and Aritoshi MASUDA[(3)]

(1) Graduate School of Engineering, Kyoto University
(2) Meteorological Satellite Center, JMA
(3) Japan Weather Association, JWA

Synopsis

The objective of this study is to investigate the relationship between RDCA index retrieved from Rapid Scan Observation (RSO) of Himawari-8 data with hydrometeor type retrieved from polarimetric radar data by considering the stage of cumulus cloud stage. The cumulus cloud life stage is retrieved from the comparison of radar-estimated cumulus life stages such as development, early mature, mature late and dissipation stage with RDCA index. We investigate seven cases of comparison of time variation between RDCA index and radar-estimated cumulus life stage. From the seven cases, we found that three cases of them have good time correlation and four others are in poor time correlation. We choose one case among the good time correlation cases and one case among the poor time correlation to investigate the relationship between RDCA index and radar-estimated hydrometeor type. We found that the poor time correlation might be due to the overestimation of RDCA index caused by the occurrence of upper-level cloud. Based on the good cases we found that there is a possibility to utilize the RDCA index to estimate the cumulus life stage.

Keywords: RDCA, GHR, baby-rain cell, RSO, Himawari-8, XRAIN

1. Introduction

Increasing hydrometeorological disasters such as flash flood caused by localized heavy rainfall is important issue in Japan recently. In Japan, the localized heavy rainfall is well known as Guerilla-heavy rainfall (GHR). The occurrence of GHR which has 30 minutes rainfall in an intensity of 50 mm/h in short rivers in urban areas in Japan has caused some tragedies, and some people died, for example, the flash flood which occurred in Toga River in Kobe in 2008. It is very important to

investigate the initiation mechanism of GHR and to predict its occurrence to secure time for people to evacuate and save their lifes. Nakakita et al. (2010) has proposed a method of detection of baby-rain cell aloft by using radar as a very important signal of GHR occurrence. Nakakita et al. (2016) identified vertical vorticity criterion in a baby-rain cell aloft to reduce failure prediction of GHR. In their case studies, GHRs can be predicted 23.6 minutes on average before rainfall reached on the ground.

To estimate the occurrence of GHR in the earlier time, we utilized the Rapid Scan Observation (RSO) of Himawari-8 observation, which provides cloud information of albedo and top surface temperature. This information may help us estimate GHR occurrence before a radar detects formation of a baby-rain cell. With this RSO observation, we used the regression model to estimate the occurrence of GHR. The model which we used is called Rapid Development Cumulus Area (RDCA) model, proposed by Satellite Meteorological Center (MSC) of Japan Meteorological Agency (JMA) and originally developed to predict lightning occurrence (Sumida et al. 2016). As lighting occurrence can be reasonably related to the development of a cloud, which can form GHRs, we directly utilize RDCA to estimate GHR occurrence in the study. The RDCA model has an output index ranging from 0.1 to 0.9, which might represent cloud development and can be used to estimate the occurrence of a GHR earlier than precipitation radar observation. Our previous work has proven that RDCA model can estimate the occurrence of GHRs 20 minutes before baby-rain cells detected by radar (Wendi et al. 2017).

To further improve the estimation accuracy of RDCA model, we would like to verify whether it could be used for revealing cumulus life stages. The RSO data, which is used to generate RDCA index just provide the information of albedo and brightness temperature of cloud at the top. Moreover, it can not give us the information about the stage of cumulus cloud development. In the verification to find the possibility of RDCA index to estimate cumulus life stage, we investigate the relationship between RDCA index with radar-estimated hydrometeor type by considering the cumulus life stage. This study becomes possible since there was a proposed method by Masuda and Nakakita (2006) which can classify the hydrometeor type and cumulus life stage.

The hydrometeor classification methodology was proposed by Masuda and Nakakita (2016) to successfully classify the types of hydrometeor aloft into eight categories such as rain, heavy rain, hail (frozen rain), big drop (big size of rain particle), graupel (small particle of snow), wet snow, dry snow and, ice crystal by using polarimetric parameters observed by X-band polarimetric RAdar Information Network (XRAIN). The classification is verified by using hydrometeor type and size of video sonde observation. Then, the information of classified hydrometeors can be used to identify the life stages of a cumulus cloud, i.e., developing, mature early, mature late, and dissipating stages in the application of matching of rain rate.

We investigated seven cases of the relationship of temporal variation between RDCA index and radar-estimated cumulus life stage. Based on the seven cases we found three of them are good correlation while other four cases show poor correlation. Thus, we compare the RDCA index and radar-estimated hydrometeor type aloft to see the relationship of precipitation and cloud condition. It is very important to investigate the capability of RDCA index for directly estimating cumulus life stages and hydrometeor type.

2. Data and Methodology

The RSO data of Himawari-8 satellite and XRAIN data are used in this study. Himawari-8, a Geostationary Meteorological Satellite was launched by the JMA locating at about 36,000 km above the equator and 140° east in the space. It not only has fine spatial and temporal resolutions, 0.5-2.0 km and 2.5 minutes, respectively (Bessho et al. 2015) but also equipped by 16 observation bands, including three visible bands, three near-infrared bands, and ten infrared bands.

XRAIN is a weather radar network installed by the Ministry of Land, Infrastructure, Transport, and Tourism (MLIT) since 2010 to fast detect localized heavy rainfall for the propose of disaster prevention. The reflectivity, Doppler velocity and four polarimetric parameters (Z_{HH}, K_{DP}, Φ_{DP}, ρ_{HV}) in the high spatial and temporal resolutions of seven X-band radars in our targeted Kinki Region shown in Fig. 1, are used to generate three-dimensional data set as shown in Table 1.

Seven cases are used to test the capability of RDCA index on estimating GHR occurrence. At the same time of the seven cases, all corresponding radar polarimetric parameters are also extracted to obtain the information of cumulus life stage and hydrometeor type by using the classification methodology (Masuda and Nakakita 2016).

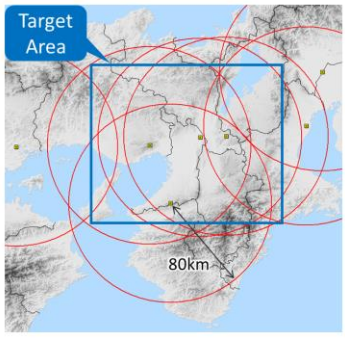

Fig. 1 Seven weather radars in Kinki

To investigate the relationship between RDCA index and radar-estimated hydrometeor we compare the RDCA index and radar-estimated cumulus life stage. After that, we compare the RDCA index and radar-estimated hydrometeor type.

Table 1 Three dimensional data

Number of radar sites	7
Horizontal grid spacing	250 m
Vertical grid spacing	500 m
Maximum altitude	10 km
Interval	1 m
Variables	R, Z_{HH}, Z_{DR} K_{DP}, ρ_{HV},

3. Result and Discussion

We choose seven cases which can estimate the occurrence of GHR using RDCA index. In the same time, we prepare the radar-estimated cumulus life stage and radar-estimated hydrometeor type. By using the seven cases, we investigate the correlation of temporal variation between RDCA index and radar estimated cumulus life stage and between radar RDCA index and radar-estimated hydrometeor type. Among the seven cases, we found three of them have good time correlation while others are in poor time correlation. In this paper, we only show one good time correlation among three good time correlations and one poor correlation among four poor time correlations.

3.1 Good correlation (3 August 2015)

3.1.1 Radar-estimated cumulus life stage

We investigate the time variation of overlaying single cumulus cloud captured by band 13 of Himawari-8's observation data and detected-rainfall in the lowest elevation from radar observation on 3 August 2015. As shown in Fig. 2, the first cloud echo is captured by Himawari-8 at 11:30 JST. Thirty

minutes after that, the first detection of rainfall in the lowest elevation of radar is detected at 12:00 JST. The T_B value decreased while the intensity of rainfall increased until 12:15 JST. The T_B decreased and the rainfall dissipated at 12:20 JST.

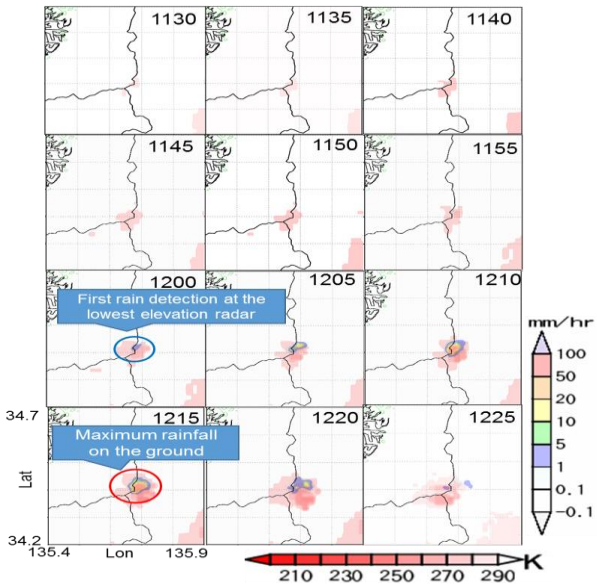

Fig. 2 Overlaying cloud echo (B13;Himawari-8) and rainfall in the lowest elevation radar observation.

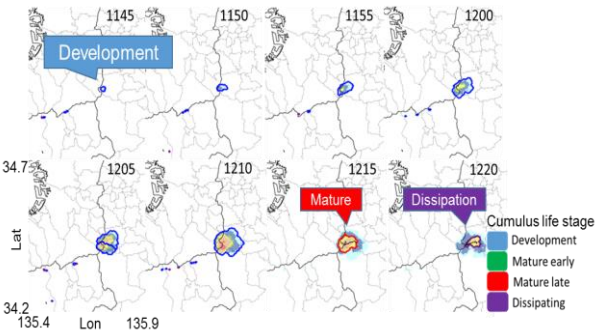

Fig. 3 Radar-estimated cumulus life stage

The cumulus life stage analyzed by radar polarimetric parameters in the same period is shown in Fig. 3. The first detection of cumulus life stage is at 11:45 JST and classified as development stage. The radar-estimated cumulus life stage changes from the development stage to mature stage at 12:15 JST. The dissipation stage is detected at 12:20 JST. We confirmed that the tendency of radar-estimated cumulus life stage is consistent with the tendency of rainfall intensity which shown in Fig. 2.

3.1.2 Comparison of RDCA index, radar-estimated cumulus life stage and radar-estimated hydrometeor type.

Fig. 4 illustrates the time variation of rainfall intensity at the lowest elevation of radar observation, RDCA index, radar-estimated cumulus life stage and radar-estimated hydrometeor type.

The first RDCA index is detected at 11:40 JST as illustrated by Fig. 4b. The RDCA index is fluctuating before the rainfall detected at the lowest elevation of radar (12:00 JST). The fluctuated of RDCA index may be due to of the fluctuation of cumulus development. The RDCA index starts to increase from 0.3 at 11:55 JST to the peak value of 0.9 at 12:10 JST. At the same time, the detected rainfall also increases. In the increasing of RDCA index and rainfall intensity, the estimated-cumulus life stage is in the development stage as shown by Fig. 4c. For this case, it is clearly evidenced that RDCA index has good time correlation with radar-estimated cumulus life stage.

In the peak of rainfall at 12:15 JST, the RDCA index also shows the top value (0.9). At this time, radar-estimated cumulus life stage is illustrated as a mature late stage. In the decreasing of rainfall intensity, the RDCA index value also decreases, and at the same time, the radar-estimated cumulus life stage is captured as dissipation stage. In this case, we confirm that the RDCA index can be used to estimate the cumulus life stage since there is a good correlation between RDCA index and radar-estimated cumulus life stage.

We generate radar-estimated hydrometeor type by using seven weather radars in Kinki region to compare with RDCA index. Since we have confirmed

that RDCA index has good correlation with radar-estimated cumulus life stage then, now we try to compare the RDCA index with radar-estimated hydrometeor type. Fig. 4d illustrates the difference of hydrometeor type in each altitude and each time.

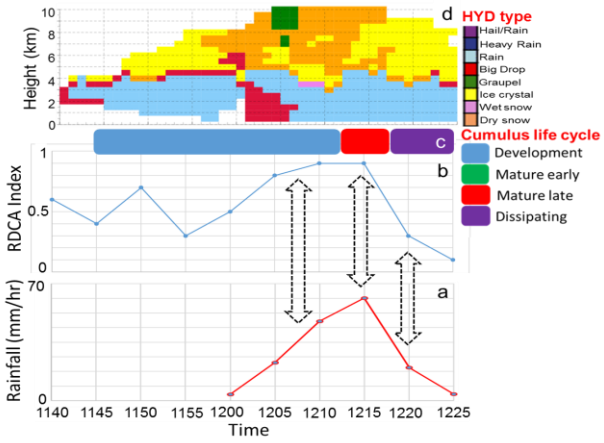

Fig. 4 Comparison of a) Rainfall intensity, b) RDCA index, c) radar-estimated cumulus life stage, and d) radar-estimated hydrometeor type.

The baby-rain cell is detected at 11:42 JST in the height of 2.75 km to 3.25 km. The type of hydrometeor in baby-rain cell stage is detected as big drop. At 11:45 JST in the height of 4.25 km the dominant hydrometeor type changes its type from big drop to rain. The type of dominant hydrometeor changes from rain to ice crystal in the height of 6.5 km at 11:50 JST. The hydrometeor is changed from ice crystal to wet snow at 12:00 JST, then change to graupel at 12:05 JST. The cumulus life stage is detected as development stage from 11:42 JST until 12:10 JST. The cumulus life stage is detected as a mature late stage at 12:15 JST when the hydrometeor is detected as dry snow. In the dissipation stage, the hydrometeor stage is detected as ice crystal.

3.2 Poor correlation (19 August 2016)

3.2.1 Radar-estimated cumulus life stage

Figure 5 shows the time variation of overlaying T_B of band 13 of Himawari-8's observation data and detected-rainfall in the lowest elevation by radar observation on 19 August 2016. The wide area of cloud is detected at 13:15 JST. The T_B value is decreasing at 13:25 JST when the radar detected the first echo of rainfall in the lowest elevation angle of its observation. Ten minutes after that, the rainfall reached its maximum value. The rainfall intensity decreased at 13:40 JST, and at the same time the T_B value is increasing which mean the cloud diminished. The rainfall intensity continues to decrease which indicates the stage of dissipation of rainfall. The wide area of cloud is still detected in the dissipation stage of rainfall. It indicates the anvil cloud or upper-level cloud occur during the dissipation stage.

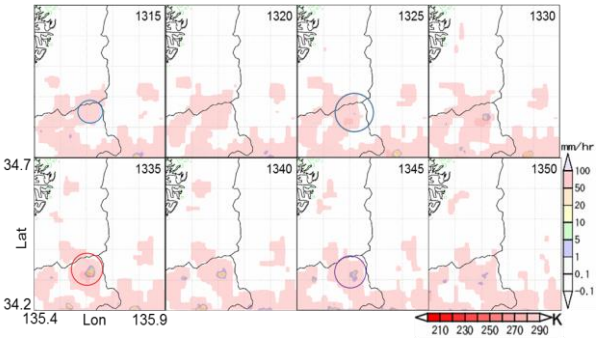

Fig. 5 Overlaying cloud echo (B13;Himawari-8) and rainfall in the lowest elevation radar observation.

The cumulus life stage generated by radar polarimetric parameter is shown in Fig. 6. The development stage detected from 13:25 JST to 13:35 JST. The radar-estimated cumulus stage changed its stage from the development stage to mature one at 13:40 JST. The estimation of cumulus life stage is different from what is shown in Fig. 5 where the maximum rainfall is detected at 13:35 JST or in another word we may say that the time estimation of cumulus life stage is not same with the time of maximum rainfall detection. The difference time indication between maximum rainfall intensity and

the estimation of cumulus life stage may be due to the temporal resolution of data. During five minutes, the cumulus life stage may be change, and rainfall intensity may reach the maximum intensity during 5 minutes.

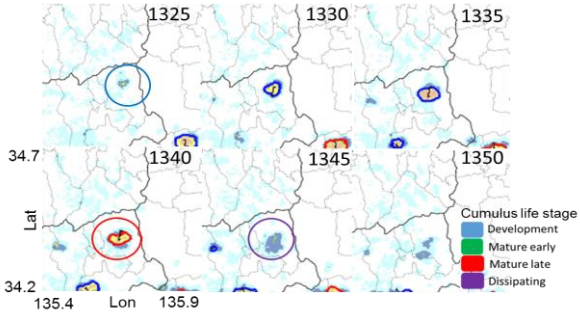

Fig. 6 Radar-estimated cumulus life stage

3.2.2 Comparison of RDCA index, radar-estimated cumulus life stage and radar-estimated hydrometeor type.

Figure 7 illustrates the comparison of the time variation of rainfall intensity at the lowest elevation of radar observation (see Fig. 7a), the RDCA index (Fig. 7b), radar-estimated cumulus life stage (Fig. 7c) and radar-estimated hydrometeor type (Fig. 7d).

The earliest detection of RDCA index is at 13:15 JST as illustrated by Fig. 7b. The RDCA index has a high value in the earliest detection and reaches its highest value (0.9) after five minutes. The RDCA index decreased at 13:30 JST from 0.9 to 0.5 and continues decreasing. At the same time, the decreasing value of RDCA index is opposite to increasing of the rainfall intensity. The radar-estimated cumulus life stage is indicated as development and mature stage during the decreasing of RDCA index. The radar-estimated cumulus life stage shows the dissipation stage in the decreasing RDCA index.

Based on the comparison between RDCA index and radar-estimated cumulus life stage we found that RDCA index does not have good correlation with radar-estimated cumulus life stage in the development and mature stages, but it has good correlation in the dissipation stage. In this case, we cannot use RDCA index to estimate cumulus life stage.

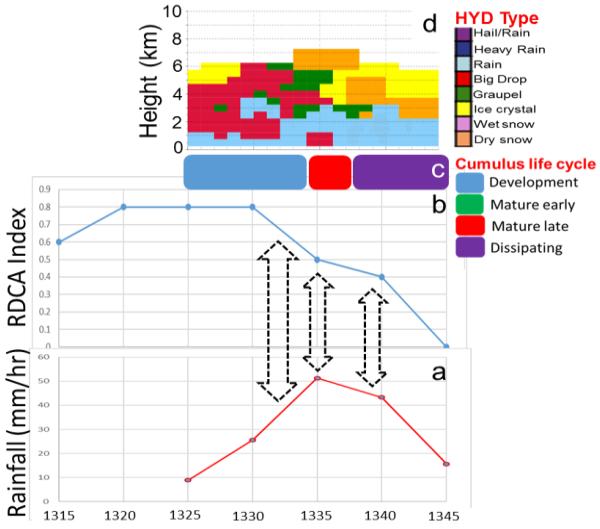

Fig. 7 Comparison of a) Rainfall intensity, b) RDCA index, c) radar-estimated cumulus life stage, and d) radar-estimated hydrometeor type.

For the poor correlation, we try to check the correlation between RDCA index and radar-estimated hydrometeor type. Fig. 7d illustrates the time and altitude variation of radar-estimated hydrometeor type. The rainfall is detected at 13:25 JST from the lowest elevation radar detection to the height 5.75 km. The hydrometeor type is detected as ice crystal at aloft. The radar-estimated hydrometeor aloft changed its type from ice crystal to the big drop. The radar-estimated cumulus life stage is detected as development stage at this time. The detection of ice crystal in the early detection of rainfall may be due to the anvil clouds which already exists before the occurrence of the lower cumulus cloud, which is also the cause of the overestimation of RDCA index.

In the mature stage of radar-estimated cumulus life state, the radar-estimated hydrometeor type is

detected as dry snow. At this stage, the RDCA index is overestimated since the Himawari-8 data cannot detect the dry snow. The Himawari-8 has only the capability to detect the cloud in the water or ice type.

The ice crystal is detected aloft in the dissipation of radar-estimated cumulus life stage. The height of ice crystal detection is decreasing in the dissipation of cloud.

4. Conclusions

We investigated the relationship between RDCA index and radar-estimated hydrometeor type considering cumulus cloud stage. By using seven cases, we compare the RDCA index with radar-estimated cumulus life stage and radar-estimated hydrometeor type. We found three cases have good correlation while four other cases are in poor correlation. The investigation of good case showed that the good time correlation might be due to the true estimation of RDCA index. The single cloud development without the existence of upper-level cloud will give the correct estimation of RDCA index. In another hand, the investigation of poor correlation showed that the occurrence of upper-level cloud or anvil cloud might be the reason of over estimation of RDCA index. Based on the good correlation we propose that Himawari-8 RSO data might be able to provide the information of cumulus life stages and hydrometeor type directly. In the future, we need to investigate more cases of the relationship between RDCA index and radar-estimated cumulus life stage to increase the capability of RDCA index in studying the development of cumulus cloud.

Acknowledgements

Thanks to the Program of Research and Innovation in Science and Technology (RISET-Pro), Ministry of Research, Technology and Higher Education (RISTEKDIKTI) of Indonesia for the scholarship which given to the main author.

References

A. Masuda and E. Nakakita, “Development of a technique to identify the stage of storm life cycle using X-band polarimetric radar,” The Journal of Japan Society of Civil Engineers, Series B, vol. 70, no. 4, pp. 493-498, 2014 (Japanese).

E. Nakakita, H. Yamabe, and K. Yamaguchi. (2010): Earlier detection of the origin of very localized torrential rainfall. *Journal of Hydraulic Engineering, Japan Society of Civil Engineers*, vol. 54, pp. 343–348. (Japanese).

E. Nakakita, H. Sato, R. Nishiwaki, H. Yamabe and K. Yamaguchi. (2017): Early detection of baby rain cell aloft in a severe storm and risk projection for urban flash flood. *Advace in Meteorology*, Article ID 5962356, 15 pages.

Harjupa, W., Nakakita, E., Sumida, Y., and Yamaguchi, K. : Fundamental Investigation of Generation of Guerilla-heavy rainfall using Himawari-8 and XRAIN information in Kinki region. *Journal of Hydraulic Engineering, Japan Society of Civil Engineers*, Vol. 74, No. 4, pp. 283-288, 2017.

K. Bessho, K. Date, M. Hayashi, A. Ikeda, T. Imai, H. Inoue, Y. Kumagai, T. Miyakawa, H. Murata, T. Ohno, A. Okuyama, R. Oyama, Y. Sasaki, Y.Shimazu, K. Shimoji, Y. Sumida. (2016): An Introduction to Himawari-8/9 - New-Generation Geostationary Meteorological Satellites, *J. Meteorol. Soc. Japan. Ser. II*, vol. 94, no. 2, pp. 151–183.

Y. Sumida, S. Hiroshi, I. Takahito and S. Akira. (2016) Meteorological Satellite Center Technical Note, no. 62.

(Received July 23, 2018)